





RESEARCH ARTICLE OPEN ACCESS

Development of Broadly Applicable Reference EVs Expressing Horseradish Peroxidase

Daniela Waas¹ | Marc Juraschitz² | Yen-Fu Adam Chen¹  | Harald Waltenberger² | Wolfgang Hammerschmidt³  | Reinhard Zeidler^{4,5}  | Sonja Molinaro² | Kathrin Gärtner¹ 

¹Eximmium Biotechnologies GmbH, Munich, Germany | ²Microcoat Biotechnologie GmbH, Bernried, Germany | ³Research Unit Gene Vectors, Helmholtz Munich, German Research Center for Environmental Health, Munich, Germany | ⁴Institute of Structural Biology, Helmholtz Munich, German Research Center for Environmental Health, Munich, Germany | ⁵Department of Otorhinolaryngology, LMU University Hospital, Munich, Germany

Correspondence: Kathrin Gärtner (kathrin.gaertner@eximmium.com)

Received: 7 August 2024 | **Accepted:** 3 June 2025

Keywords: extracellular vesicles | horseradish peroxidase | normalization | quality control | standardization

ABSTRACT

Extracellular vesicles (EVs) hold great promise as circulating biomarkers for diagnostic and therapeutic approaches. Thus, many research groups world-wide investigate important aspects of EVs including their biology and medical significance. For this, a large number of procedures and protocols has been established making it difficult to almost impossible to compare and replicate results. Consequently, diagnostic tests remain problematic to interpret, mainly because the use of reliable reference EVs as a qualified standard has not yet gained widespread acceptance. Beyond doubt, such reference EVs are key to assess EV preparations quantitatively and to establish robust quality control processes to ensure overall quality and validity of data. To further advance the establishment of such controls, we designed and generated a new class of reference EVs expressing horseradish peroxidase (HRP) to facilitate simple and reliable EV tracing during isolation and standardization of EV purification and downstream analysis processes. HRP⁺ EVs can be quantified easily and with unmatched sensitivity either directly via measuring HRP activity or indirectly via immunodetection of HRP on the EV surface. We demonstrate that HRP⁺ EVs allow the reliable quantification of absolute EV numbers in biological or medical samples to normalize clinical specimens in liquid biopsies.

1 | Introduction

Extracellular vesicles (EVs) are nanosized particles secreted by all types of cells and thus present in cell culture samples and body fluids such as serum, plasma, urine and cerebrospinal fluids. EVs consist of a lipid bilayer encompassing a luminal cargo that contains functional proteins, nucleic acids and metabolites. As EVs are released from very different cell types, content and composition of EVs resemble their cellular origins making them useful conveyors of biological information, which can be explored in various scenarios (Théry et al. 2002; Van Niel et al. 2018).

EVs are found to be implicated in various physiological processes but also pathological conditions, that is, cancer, acute and chronic infection, and degenerative cellular processes and diseases. Cancer cell-derived EVs have been described to, for example, activate or recruit cancer or stromal cells locally and to educate premetastatic niches at distant locations, thereby fostering metastasis formation (Becker et al. 2016; Li et al. 2019; Zhang et al. 2024). EVs isolated from different biofluids have been found to contain specific mRNA, miRNA and proteins related to disease state for breast, urogenital, pancreatic and ovarian cancer (Melo et al. 2015; Nawaz et al. 2014; Sadovska et al. 2015; Tang and Wong 2015).

This is an open access article under the terms of the [Creative Commons Attribution-NonCommercial-NoDerivs](https://creativecommons.org/licenses/by-nc-nd/4.0/) License, which permits use and distribution in any medium, provided the original work is properly cited, the use is non-commercial and no modifications or adaptations are made.

© 2025 Eximmium Biotechnologies GmbH. *Journal of Extracellular Vesicles* published by Wiley Periodicals LLC on behalf of International Society for Extracellular Vesicles.

Utilizing EVs as circulating biomarkers of disease holds a lot of promise for non-invasive diagnostics, also referred to as 'liquid biopsy'. However, little advances have been made toward routine clinical applications and identification of reliable EV-associated diagnostic markers remains challenging. This is also because EV research is difficult to reproduce owing to the plethora of isolation methods used in the field. Experimental standards and processes have been proposed but normalization of data across publications is tedious or uncertain (Théry et al. 2018; Van Deun et al. 2017; Witwer et al. 2013). In essence, both the clinical usage as well as scientific progress in the field are significantly hampered by poorly established use of reliable, easy-to-use reference EVs that allow for intra- and inter-experimental normalization and standardization.

Currently, various biological and biophysical reference EVs and particles are available. They are either derived from biological sources, such as virus particles and liposomes, often equipped with a fluorophore (Geeurickx et al. 2019; Valkonen et al. 2017; Welsh et al. 2020), or they are made of artificial materials such as polystyrene or silica, thus having different biochemical properties compared to naturally occurring EVs (Varga et al. 2018; Wang et al. 2008). Fluorescent reference EVs are usually derived from cell culture supernatants and can be used for standardization of samples and calibration of fluorescence-based instruments, that is, nanoflow cytometry or fluorescent nanoparticle tracking analysis (F-NTA) (Geeurickx et al. 2021; Görgens et al. 2019). However, low sensitivity, instability and photobleaching can significantly limit the application of fluorescence-based reference EVs.

To overcome these limitations and to complement the range of existing reference material, we introduce a new class of reference EVs carrying a recombinant horseradish peroxidase (HRP), an enzyme derived from horseradish roots (*Amoracia rusticana*), anchored to the EV surface. Among peroxidases, particularly HRP has conquered a prominent position and has been studied for more than a century (reviewed in Azevedo et al. 2003; Krainer and Glieder 2015; Veitch 2004). HRP-based detection systems are nowadays widely used in research and biotechnological industries, for example, as antibody conjugates in immunochemical applications such as ELISA, immunohistochemistry, and Western blotting.

HRP catalyses the reaction of hydrogen peroxide with electron-donating substrates to form intensely coloured products, which can be detected by chemiluminescent, fluorometric and colorimetric methods. HRP is characterized by its small size, high stability and a high turnover rate. Commonly used substrates like luminol, tyramine, 3,3',5,5'-Tetramethylbenzidine (TMB), 3-amino-9-ethylcarbazole (AEC) and 3,3'-diaminobenzidine (DAB) are catalysed into stable accumulating products that allow a very sensitive and relatively fast signal detection. Together, these features make HRP an attractive and useful enzyme for reference EVs.

In the present study we show that HRP⁺ EVs derived from an engineered, stable HEK293-derived cell line can be easily detected and tracked enzymatically and immunologically and are suitable for normalization of endogenous EVs contained in various biological specimen.

2 | Material and Methods

We have submitted all relevant data of our experiments to the EV-TRACK knowledgebase. EV-TRACK ID: EV250062 (Van Deun et al. 2017).

2.1 | Cell Culture

A HEK293 cell line adapted to high-density suspension growth was kindly provided by Josef Mautner, Helmholtz Munich, Germany. Stable expression of HRP was achieved by retroviral transduction followed by column-based magnetic cell sorting (MACS MicroBeads Technology, Miltenyi Biotec, Bergisch Gladbach, Germany). HRP expression on the cell surface was measured by flow cytometry (BD Canto, Becton Dickinson GmbH, Heidelberg, Germany) using an HRP-specific antibody (ab10183, Abcam, Cambridge, UK). The HRP⁺ EV-producing cells were adapted to grow in serum-free, synthetic medium (LV-MAX Production medium, Thermo Fisher). One micrometre of hemin (H9039, Sigma-Aldrich, Taufkirchen, Germany) was added to the medium to ensure HRP functions. Cell viability was checked by trypan blue exclusion and cultures with viabilities above 95% were used for experiments.

2.2 | Isolation of EVs From Conditioned Medium

Cells were seeded at a concentration of 2×10^6 cells/mL and incubated in synthetic medium for 72 h. The supernatant was harvested and centrifuged in two sequential runs (10 min at $300 \times g$, 4°C, and 20 min at $5000 \times g$, 4°C) to remove cells and debris, respectively. After filtration of the supernatant (pore size 0.8 µm) EVs were collected by sedimentation after ultracentrifugation ($100,000 \times g$, 2 h, 4°C) in a SW32 swing-out rotor (Beckman Coulter, CA, USA). Pellets were resuspended in PBS (PAN Biotech, Aidenbach, Germany) supplemented with protease inhibitors (cOmplete Mini, EDTA-free, Roche, Basel, Switzerland). Particle concentration of EV samples was determined by nanoparticle tracking analysis (NTA) using the ZetaView PMX110 instrument (Particle Metrix, Inning, Germany). In Figures 1D, 2B and S6, HRP⁺ EVs were further purified by flotation gradient ultracentrifugation in a 4-mL two-layer bottom-up iodixanol (Optiprep, Sigma-Aldrich) gradient using a SW60Ti swing-out rotor ($160,000 \times g$, 16 h, 4°C), as described in Gärtner et al. (2019). Briefly, 500 µL of EVs were mixed with iodixanol to reach a final concentration of 44%, and carefully overlayed in 4-mL tubes (Ultra-Clear Thinwall, Beckman Coulter) with 2.3 mL 30% iodixanol and 600 µL PBS. The gradient was centrifuged for 16 h at $160,000 \times g$ at 4°C. Subsequently, eight fractions of 500 µL each were collected from the top, and their specific densities were measured with a refractometer (Reichert Technologies, Unterschleißheim, Germany).

2.3 | Nanoparticle Tracking Analysis

EVs were enumerated by NTA using the ZetaView PMX110 instrument (Particle Metrix, Inning, Germany) and its corresponding software (ZetaView 8.02.31). The instrument was calibrated with polystyrene beads of known size and concentration (100 nm

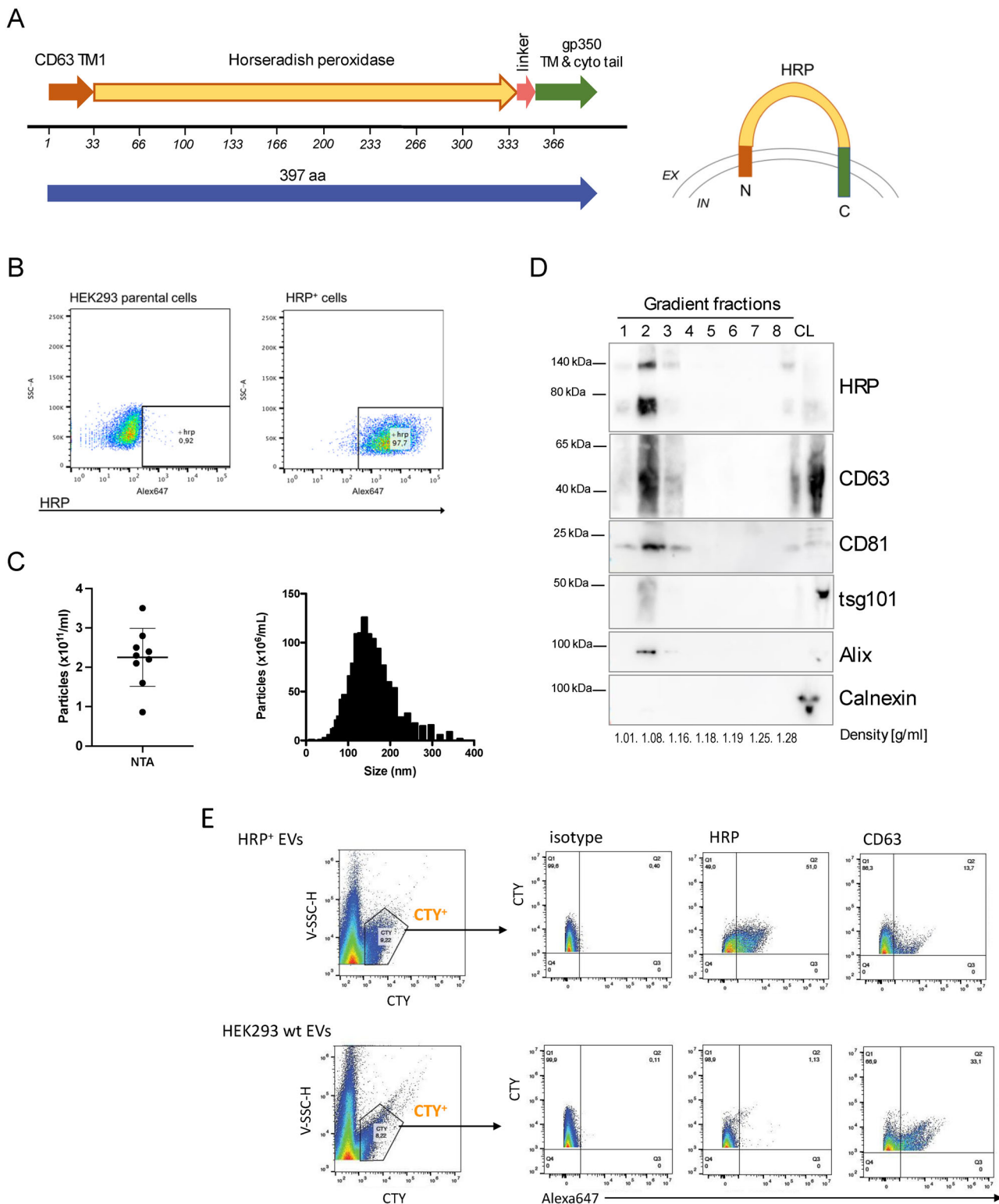


FIGURE 1 | Legend on next page.

NanoStandards, Applied Microspheres, Leusden, The Netherlands). Purified EVs were diluted in PBS to a concentration of 100–200 particles per video frame. Each EV sample was measured at 11 positions with three reading cycles at each position. Temperature was kept constant throughout the measurement at

22°C. The pre-acquisition parameters were set to a sensitivity of 75, a shutter of 50, a frame rate of 30 frames per second and a trace length of 15. The post-acquisition parameters were set to a minimum brightness of 20, a minimum size of five pixels and a maximum size of 1000 pixels.

2.4 | Immunoblotting

Density gradient fractions (Figure 1D) or purified HRP⁺ EVs (Figure 3D) were mixed with 5x Laemmli protein sample buffer and boiled for 10 min at 95°C. Corresponding cell lysates were prepared with ice-cold RIPA lysis buffer. Protein samples were resolved on 4–12% bis-tris/acrylamide gels (Thermo Fisher), blotted onto nitrocellulose membrane (GE Healthcare, IL, USA) followed by blocking for 1 h in 5% non-fat milk and incubation with primary antibodies at 4°C under constant shaking overnight. The membrane was washed in TBS/0.05% Tween-20, incubated with HRP-coupled secondary antibodies at room temperature for 2 h and finally developed with electro chemiluminescence (ECL). Signals were quantified on a Vilber Fusion FX6 (Marne-la-Vallée, France). The following detection antibodies were used: mouse anti-HRP (1:1000, ab10183, Abcam), rat anti-CD63 (24F9, Core Facility Monoclonal Antibodies, Helmholtz Munich, Germany), mouse anti-CD81 (1:1000, B-11, ab10183, Santa Cruz Biotechnology, CA, USA), mouse anti-tsg101 (1:1000, 4A10, GeneTex, Irvine, CA, USA), mouse anti-Alix (1:500; 3A9, BioLegend, London, UK), and mouse anti-Calnexin (1:1000, 610523, BD Biosciences, Heidelberg, Germany). HRP-labelled secondary antibodies were purchased from Jackson ImmunoResearch (PA, USA). Non-reducing sample buffer without β -mercaptoethanol was used for the detection of CD63.

2.5 | Electron Microscopy

For negative staining, 5 μ L of an EV sample was applied onto continuous carbon grids (CF300-CU Electron Microscopy Sciences) after glow discharging for 30 s. After 60 s the sample was then blotted of with filter paper and the grid was quickly washed with 20 μ L HEPES buffer (1M). Immediately after washing, 5 μ L of 1% uranyl acetate solution were added and removed with a filter paper after 30 s. Grids were then transferred into a JEM-1400Plus transmission electron microscope (JEOL, Freising, Germany) operated at 120 kV and imaged at a nominal magnification of 20k. Images were taken with a Ruby CCD camera (JEOL) with a final pixel size of 0.81 nm/px.

2.6 | Flow Cytometry Analysis of EVs

To analyse purified HRP⁺ EVs by high-sensitive flow cytometry, their lumen was first stained with the dye CellTrace Yellow (Thermo Fisher, MA, USA). Briefly, 400 μ L of EV preparations (approx. 1×10^{11} EVs/mL) were mixed with 2 μ L of CellTrace Yellow (CTY) and incubated at 37°C for 20 min. To remove excess dye, 10 mL of PBS/1% BSA was added, and the suspension was transferred to a Amicon Ultra-15 centrifugal filter (Merck, Darmstadt, Germany) with 100 kDa molecular weight cutoff. After two rounds of centrifugation at $2000 \times g$ for 15 min, the retentate, containing the CTY-labelled EVs (~500 μ L) was transferred into a fresh vial. The EV preparations were stained with the directly coupled antibodies anti-HRP-Alexa647 (323-605-021, Jackson ImmunoResearch), anti-CD63-Alexa647 (Core Facility Monoclonal Antibodies, Helmholtz Munich, Germany), or an isotype control antibody. For this, 50 μ L of CTY⁺ EVs were mixed with 0.5 μ L of antibody and incubated on ice for 30 min. Controls comprised buffer controls without EVs and unstained EV samples for the antibody staining.

Prior to measurement, the samples were further diluted 1:1000 in PBS. They were analysed by high-sensitivity nanoflow cytometry using a CytoFLEX instrument (Beckman Coulter, CA, USA) with the following settings: trigger on 405 nm violet side scatter (V-SSC), violet side scatter detection set to 500, slow speed setting for 3 min (flow rate 10 μ L/min). Gain settings were: 60 for V-SSC, 850 for APC and 950 for PE. Between each sample, the sample line and flow cell were washed thoroughly for 2 min with 80% EtOH and PBS.

2.7 | Treatment of EVs With Proteinase K

Purified HRP⁺ EVs were treated with 20 μ g/mL of the broad-spectrum serine Proteinase K (PK; New England Biolabs, Frankfurt) and 5 mM CaCl₂ for 1 h at 37°C to digest proteins exposed on the EV surface. The PK activity was inhibited by adding 5 mM PMSF (10 min at room temperature). CaCl₂ and PMSF, but no PK, were added to the control sample.

FIGURE 1 | Generation and characterization of EVs containing membrane-tethered horseradish peroxidase. (A) The HRP fusion protein is composed of a central domain with a codon-optimized HRP coding sequence flanked by an N-terminal domain derived from the first transmembrane domain of the human CD63 protein and the C-terminal transmembrane (TM) and cytoplasmic tail (cyto tail) of the EBV glycoprotein gp350. A linker sequence composed of a stretch of serine and glycine residues connects the HRP and gp350 sequences. Scale numbers indicate amino acid residues. The illustration on the right represents the presumed orientation of the fusion protein in the EV membrane. TM, transmembrane domain; cyto tail, cytoplasmic domain of gp350; EX, extraluminal; IN, intraluminal; C, C-terminus; N, N-terminus. (B) Expression of the HRP fusion protein on the surface of a stably transduced HEK293 suspension cell line, HEK293-HRP⁺, was measured by flow cytometry using an Alexa647-coupled HRP-specific antibody (right panel) and compared to parental HEK293 cells (left panel). SSC-A: area of sideward scatter; numbers within the gates: percentage of HRP-positive cells. (C) After 3 days of cultivation in serum-free medium, the conditioned medium of HEK293-HRP⁺ suspension cells was harvested and EVs were purified by serial centrifugation, including ultracentrifugation. Nine independent HRP⁺ EV preparations were analysed. Nanoparticle tracking analysis was used to determine the concentration (left panel) and size distribution (right panel) of the concentrated EVs. The size distribution of one representative sample is shown and the mean size was found to be 149 nm. (D) HRP⁺ EVs were further purified by floating density gradient centrifugation using iodixanol gradients. The fractions were analysed by Western blotting. EVs expressing HRP and the EV-enriched proteins CD63, CD81, tsg101 and Alix were mainly detected in fraction 2. HRP and CD63 were detected by using non-reducing conditions. CL: cell lysate. (E) Gradient-purified and enriched EVs from supernatants of HRP-expressing HEK293 cells and wildtype parental cells were tested for expression of surface HRP and CD63 by nanoflow cytometry using a CytoFLEX instrument. To discriminate EVs from background events, EVs were stained with an intraluminal dye, CellTrace Yellow (CTY), prior to antibody staining. The gates in the two leftmost panels demark CTY-positive EVs in the preparation. The shown experiment is representative for three biological replicates.

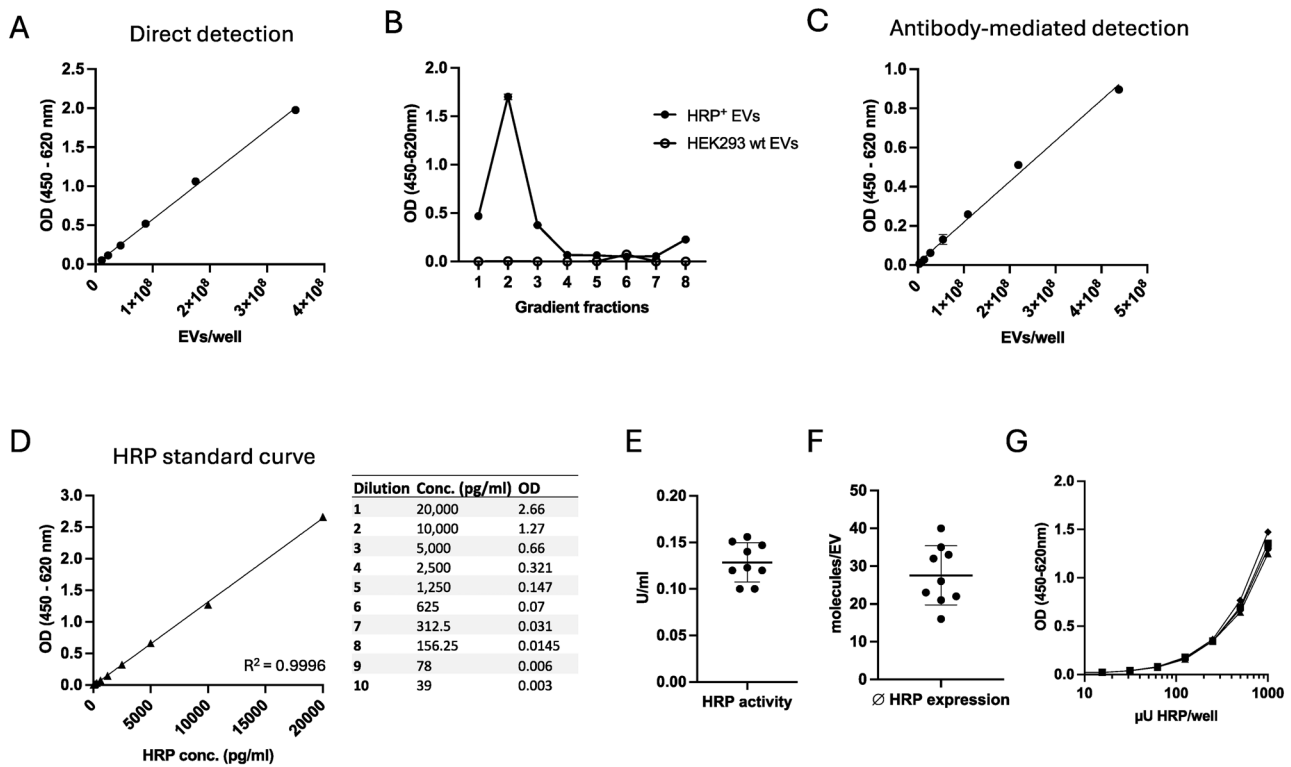


FIGURE 2 | Characterization and detection of EV-associated HRP activity. (A) HRP⁺ EVs were purified from conditioned medium of HEK293-HRP⁺ cells by serial centrifugation including ultracentrifugation (UC) and diluted in PBS as indicated. HRP activity was measured directly by colorimetric detection of the catalysed TMB substrate, the reaction was stopped after 10 min with 0.5 M H₂SO₄. Data points indicate mean of triplicates. $R^2 = 0.9978$. (B) To demonstrate the co-purification and physical linkage of the HRP enzyme and HRP⁺ EVs, the purified EVs were loaded underneath a preformed iodixanol density gradient. As control, EVs from wildtype HEK293 cells were used. After ultracentrifugation eight fractions were collected from top to bottom and HRP activity was measured in 1 μ L of each fraction diluted in 50 μ L PBS in a 96-well plate after addition of TMB substrate to each well. The reaction was stopped after 10 min. (C) HRP activity of EVs was measured after antibody-mediated immobilization of UC-purified HRP⁺ EVs. Substrate turnover was stopped after 15 min. Data points indicate mean of triplicate samples. $R^2 = 0.9947$. (D) Purified HRP enzyme from a commercial vendor with known concentration of HRP activity was diluted in PBS as indicated. The absorbance was measured by adding TMB substrate, the reaction was stopped after 5 min. $R^2 = 0.9996$. (E) The enzymatic activity was determined by diluting UC-purified HRP⁺ EVs 1:500 in PBS prior to adding TMB. ODs were measured in parallel with the HRP standard as demonstrated in panel A on the same 96-well cluster plate and the standard curve's equation was used to calculate the enzymatic activity of the EV samples; Nine individual samples were analysed. (F) The HRP enzyme standard was used to calculate the average number of HRP molecules per EV in the nine EV preparations of panel E. (G) To confirm our quantitative analyses of HRP activities in different independent preparations, four HRP⁺ EV samples, as analysed in panel E, were diluted to obtain a series of calculated HRP concentration from 10 to 1000 μ U/well. Absorbance was measured on the same plate after adding TMB substrate.

2.8 | Detection of EV-Associated and Free HRP Using the TMB Substrate

HRP⁺ EV samples and dilutions of purified HRP enzyme (263 U/mg, 31490, Thermo Fisher) were detected by using the colorimetric TMB substrate (BD OptEIA, BD Biosciences). Briefly, the samples were diluted in PBS to the required concentration and 50 μ L per well were transferred to a 96-well microtiter plate (Nunc MaxiSorp, Thermo Fisher). Subsequently, 50 μ L of TMB substrate was added per well and substrate turnover was stopped with 50 μ L of 0.5 M H₂SO₄ after 5–60 min. Absorbance was measured on a CLARIOstar plate reader (BMG Labtech, Ortenberg, Germany) at 450 and 620 nm (reference wavelength).

To detect HRP by antibody-mediated immobilization, 96-well plates were coated overnight at 4°C with an HRP-specific antibody (5 μ g/mL, ab10183, Abcam) diluted in PBS. On the

next day, the plate was washed four times with wash buffer (TBS/0.05% Tween-20) and blocked for 2 h in 5% non-fat milk at 37°C. Afterward samples containing HRP⁺ EVs were added and incubated for 2 h at 37°C. The plate was washed again to remove unbound EVs and HRP activity was measured by adding TMB substrate.

2.9 | Detection of EV-Associated and Free HRP Using the Amplex Red Substrate

HRP⁺ EV samples and dilutions of purified HRP enzyme were detected by using the fluorogenic Amplex UltraRed reagent (Invitrogen). Amplex Red was dissolved in DMSO to prepare a 10 mM stock solution. Prior to use, Amplex Red was further mixed with PBS and 3% hydrogen peroxide, according to the manufacturer's protocol. This solution was used within 4 h as HRP substrate.

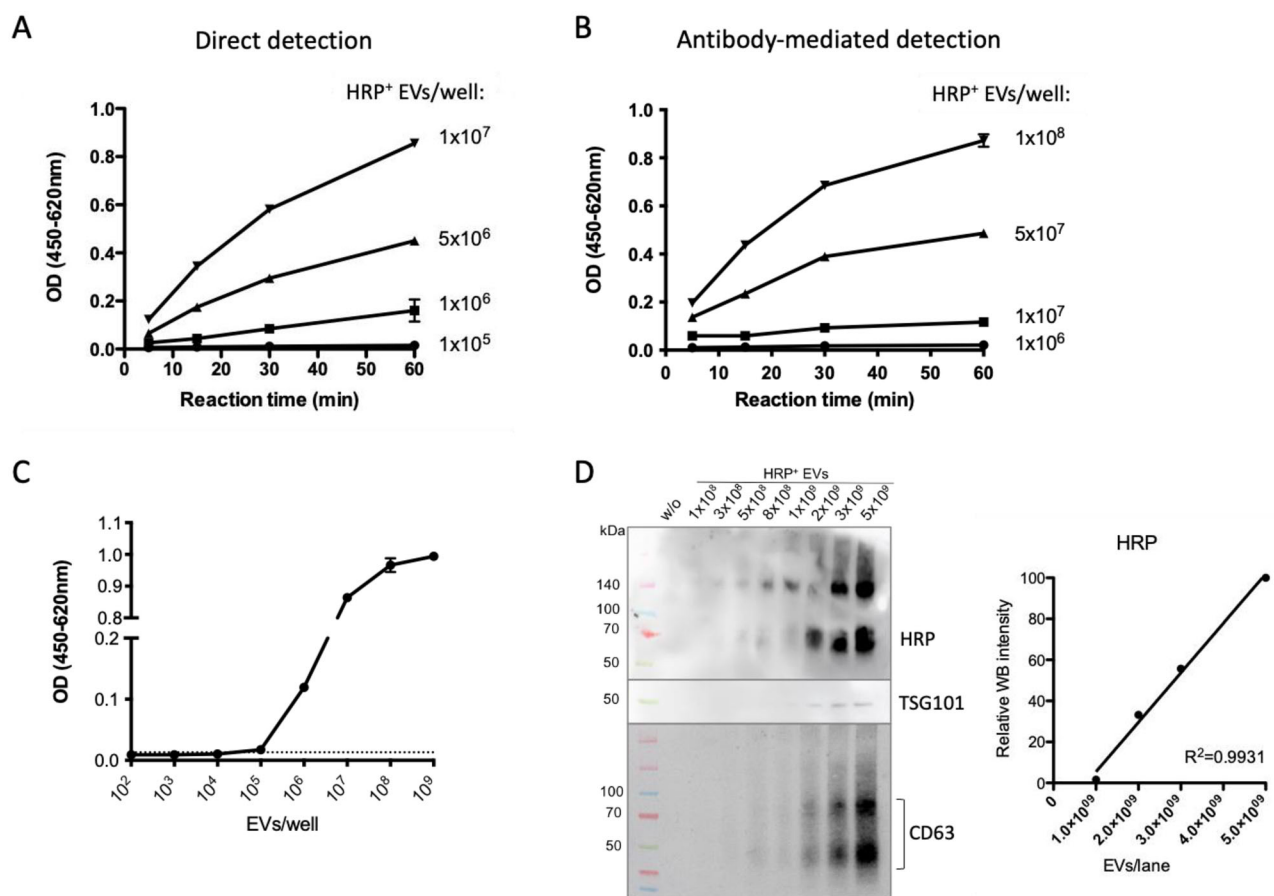


FIGURE 3 | Sensitivity of HRP detection using HRP⁺ EVs. (A) Indicated numbers of HRP⁺ EVs were diluted in PBS in triplicates in a total volume of 50 μ L and were transferred to a 96-well cluster plate. 50 μ L TMB was added to each well and the reaction was stopped after 5, 15, 30 or 60 min with 0.5 M H₂SO₄. (B) The EVs were immobilized with an HRP-specific antibody (5 μ g/mL) and HRP activity of bound EVs was measured by adding TMB substrate. Turnover of TMB was stopped at the indicated time points. (C) HRP⁺ EVs were serially diluted, and the absorbance was measured by adding TMB for 60 min. The dotted line indicates the lower limit of detection based on the value of the standard deviation of the blank value multiplied by the factor 3. (D) EVs were diluted in PBS and different amounts per lane were loaded and analysed by Western blot immunodetection using antibodies that detect the indicated proteins HRP, TSG101 and CD63. Signal intensities of HRP were determined using the ImageJ software and were plotted against absolute EV numbers tested. $R^2 = 0.9931$.

HRP-containing samples and controls were diluted in PBS to the required concentration and 50 μ L per well were transferred to a white 96-well microtiter plate (Nunc MaxiSorp, Thermo Fisher). Subsequently, 100 μ L of Amplex Red substrate solution were added per well and the plate was incubated protected from light. For most reactions, a 10–30-min incubation is sufficient. Fluorescence was measured on a CLARIOstar plate reader.

2.10 | Detection of HRP-Specific mRNA by RT-qPCR

RNA from purified EVs was isolated using the RNeasy Mini Kit (Qiagen, Hilden, Germany) according to the manufacturer's instructions and then transcribed into cDNA with the QuantiTect Reverse Transcription Kit (Qiagen). Quantitative PCR was performed using the LightCycler 96 instrument (Roche) with two detection methods: LightCycler 480 SYBR Green I Master for amplification of the housekeeping gene GAPDH and PrimeTime Gene Expression Master Mix with FAM 520 5' reporter dye and ZEN/Iowa Black FQ quencher (Integrated DNA Technolo-

gies, Coralville, IA, USA) for HRP detection. The following primers and probes were used: GAPDH forward 5'-CTTGTCAA GCTCATTTCTGG-3' and reverse 5'-TCTTCTCTTGCTCT TGC-3'; HRP forward primer 5'-CGACCAGGAGCTGTTTC TAG-3'; reverse primer 5'-GAATGTCTGGGTAGAGTTGGC-3' and probe 5'-ATTGTATCGGTGGCGTTGGGC-3'.

2.11 | Isolation of EVs From Serum

Serum samples from healthy donors were purchased from the BioIVT biobank (Glasgow, UK) and stored at -20°C . For EV isolation, serum samples were thawed and centrifuged at $300 \times g$ for 10 min and at $16,000 \times g$ for 30 min to remove cellular debris and thrombocytes. To evaluate the use of HRP⁺ EVs as internal reference control, sera were spiked with HRP⁺ EVs prior to commonly used isolation methods.

Size exclusion chromatography (SEC) was performed using the qEVoriginal columns (70 nm, Izon Science, Lyon, France), according to the manufacturer's protocol. Briefly, the SEC column

was first equilibrated with PBS. Then 500 μ L of serum was loaded onto the loading frit of the column and fractions of 500 μ L were collected. EV-rich fractions were pooled, as indicated in Figure S1.

EVs were also isolated from sera by using mini spin columns (69725, Thermo Fisher) pre-packed with 1 mL of CL-4B Sepharose (CL4B200, Sigma-Aldrich) slurry. One hundred microlitres of serum was loaded on top of the sepharose-containing spin column placed in a 1.5-mL microcentrifuge tube and incubated at room temperature for 5 min. The tube was then centrifuged at $50 \times g$ for 3 min and the flow-through was discarded. The column was placed into a fresh microcentrifuge tube and 150 μ L of PBS was added on top of the sepharose. After centrifugation for another 3 min, the EV-containing fraction was collected. To verify the successful separation of EVs and proteins (as indicated in Figure S2), the procedure was repeated twice by adding another 150 μ L of PBS on top of the spin column. The particle numbers and the protein concentrations of the four fractions were measured by NTA and BCA protein assay (Thermo Fisher), respectively.

Serum EVs were furthermore isolated with the commercial Exo-Quick ULTRA kit for serum and plasma (System Biosciences, CA, USA) and ExoSpin mini kit (Cell Guidance Systems, Cambridge, USA), according to the manufacturer's instructions.

3 | Results

3.1 | Generation and Characterization of EVs Expressing Functional HRP on Their Surface

To obtain EVs carrying HRP as an ectoenzyme (HRP⁺ EVs), the cDNA was cloned into a suitable expression plasmid in frame with a N-terminal transmembrane (TM) domain derived from CD63 and a C-terminal TM domain derived from the Epstein-Barr virus (EBV) glycoprotein gp350 (Figure 1A). A HEK293 suspension cell line was stably transduced with a retroviral vector and cells expressing the HRP fusion protein on their surface (HEK293-HRP⁺) were selected by column-based magnetic cell sorting and an antibody directed against HRP. Expression of high levels of surface HRP was confirmed by flow cytometry (Figure 1B). To avoid contamination with EVs contained in foetal calf serum, the HRP⁺ EV-producing cells were adapted to serum-free, synthetic medium containing 1 μ M of hemin, the co-factor of HRP (Figure S3).

After 3 days of cultivation of HEK293-HRP⁺ cells in serum-free medium, EVs were isolated from 30 mL of conditioned supernatant by serial centrifugation. Particle concentration and size distribution of EVs contained in the $100,000 \times g$ pellet were analysed by NTA (Figure 1C). Analysis of the HRP⁺ EVs by electron microscopy demonstrated that the isolated material contained round, cup-shaped membrane vesicles of a diameter of 100–200 nm (Figure S4). We also compared the mean size of HRP⁺ EVs (137.3 ± 7.8 nm, $n = 20$) to EVs isolated from serum, wildtype HEK293 cells or various cancer cell lines (Figure S5A) and did not observe significant differences on the 0.01 significance level, except for the HepG2 cell line ($p = 0.0024$; Mann-Whitney test). HRP⁺ EVs and HEK293-wt EVs also showed a similar zeta potential with -40.92 ± 2.63 mV and -41.87 ± 4.30 mV, respectively (Figure S5B).

We then purified the EVs by flotation density gradient centrifugation using a pre-formed iodixanol gradient. Eight fractions were collected, and Western Blot analysis showed that HRP co-localized with the EV marker proteins CD63, CD81, tsg101 and Alix mainly in fraction 2, corresponding to a buoyant density of 1.08 g/mL (Figure 1D). The HRP appears as a highly glycosylated double band due to dimerization under non-reducing conditions. Indicative for the purity of the EV preparations, calnexin, a protein of the endoplasmic reticulum, was absent from all fractions. Additionally, particle numbers and protein concentrations in all fractions were measured by NTA and BCA protein assays, respectively (Figure S6).

To analyse whether HRP was located on the surface of EVs, we co-stained EVs isolated from fraction 2 with a fluorescent dye (CellTrace Yellow) and antibodies specific for HRP or CD63 and coupled with Alexa-647, to analyse them by high-sensitive nanoflow cytometry (Figures 1E and S7). Gradient purified EVs from wildtype HEK293 cells were used as control. A large fraction of EVs derived from HEK293 cells expressing HRP carried the protein on their surface whereas EVs released from parental HEK293 cells were negative.

3.2 | Measurement and Quantification of EV-Associated HRP

We next analysed the enzyme's functionality in EV samples using two independent methods (Figure 2). First, we determined the enzymatic activity by adding the HRP substrate TMB directly to a serial dilution of purified HRP⁺ EVs followed by measuring substrate turnover colorimetrically. The absorbance measured at 450 nm revealed a linear correlation with the number of HRP⁺ EVs within the depicted range of 1×10^7 – 3.5×10^8 EVs/well (Figure 2A). A similar result was obtained when the fluorogenic HRP substrate Amplex Red was used, indicating that EV-associated HRP can be detected by various commercially available substrates (Figure S9A).

HRP-specific signals could also be detected by directly adding TMB substrate to fractions of an iodixanol density gradient. In line with the Western blot results in Figure 1D, the HRP signal was mainly detected in fraction 2 of the gradient, confirming the specific co-purification of the enzyme with EVs (Figure 2B). As a second read-out, a 96-well cluster ELISA plate was coated overnight with an HRP-specific antibody (5 μ g/mL, ab10183, Abcam). After washing and blocking of the wells to avoid unspecific binding, different numbers of EVs diluted in PBS were added to the wells and incubated for 2 h. After washing to remove unbound EVs, TMB was added to the wells, and the HRP activity was measured colorimetrically. This antibody-mediated detection revealed a linearity in the range of 1×10^7 – 4.5×10^8 EVs/well (Figure 2C). When we treated purified HRP⁺ EVs with Proteinase K prior to measuring the HRP activity directly or after antibody-mediated immobilization, we observed complete disappearance of the HRP signal, whereas EV integrity, measured by NTA, was not affected (Figure S8). This confirms one more time the surface association of the HRP enzyme.

To further quantify active HRP on the surface of HRP⁺ EVs, we established an assay based on commercially available, purified

HRP enzyme of a defined enzymatic activity. An example of a standard curve is shown in Figure 2D, which demonstrates a linear range of substrate turnover from 40 to 20,000 pg HRP/mL. A similar standard curve could also be generated by using the fluorogenic substrate Amplex Red (Figure S9B).

We used the HRP standard curve to calculate the enzymatic activity contained in nine biological and technical replicates of purified HRP⁺ EVs from conditioned medium of HEK293-HRP⁺ cells. The isolated EVs had an average HRP activity of 0.13 ± 0.02 U/mL (Figure 2E) and a particle concentration of $2.6 \pm 0.74 \times 10^{11}$ /mL, as determined by NTA. We also determined the number of HRP molecules per EV using the external HRP standard and the nine EV preparations as above. The HRP enzyme has a molecular weight of 44.1 kDa, which corresponds to 1.37×10^{16} molecules contained in 1 mg of HRP enzyme. Given the known particle concentration as determined by NTA and the unit definition of HRP activity in HRP⁺ EV samples (according to the external HRP protein standard as in Figure 2E), the number of HRP molecules per particle can be calculated. As shown in Figure 2F, the nine HRP⁺ EV preparations contained 26 functionally active HRP molecules per EV on average.

To challenge the accuracy of our calculations, we selected four HRP⁺ EV preparations shown in Figure 2E. Based on their individual, lot-specific HRP activities, we did serial dilution of the four HRP⁺ EV preparations ranging from 10 to 1000 μ U per well and measured the dose-dependent turnover of TMB. The congruency of the curves in Figure 2G confirmed the consistent correlation between enzyme units and photometric absorbance of TMB substrate turnover in all batches tested.

3.3 | Detection of EV-Associated HRP Is Highly Sensitive

We next assessed the lower limit of detection (LLoD) by measuring the enzymatic activity in a serial dilution of HRP⁺ EVs (1×10^5 – 1×10^7 EVs/well). The turnover of TMB was stopped at different time points by adding 0.5 M sulfuric acid as indicated in Figure 3A. This assay revealed a LLoD of 1×10^6 HRP⁺ EVs. The HRP⁺ EVs were also measured after immobilization to an HRP-specific antibody (Figure 3B). In this experimental setup, the LLoD was 1×10^7 HRP⁺ EVs indicating that immobilization of the HRP⁺ EVs using an HRP-specific antibody reduced the overall sensitivity of detection. In Figure 3C, a serial logarithmic dilution of HRP⁺ EVs was incubated with TMB for 60 min. The LLoD (dotted line) was calculated to be 1×10^5 HRP⁺ EVs considering three standard deviations above the mean of the blank.

The HRP protein in HRP⁺ EVs can also be detected by Western blot immunodetection, as shown in Figure 3D. The signal density of the Western blot bands showed a linear correlation within a range of 1×10^9 – 5×10^9 HRP⁺ EVs.

3.4 | HRP⁺ EVs Are Stable During Storage and in Complex Biological Samples

To investigate the stability of HRP⁺ EVs stored under different conditions and for variable periods of time we first stored EVs in

PBS at 4°C for up to 7 days in three biological replicates. Despite a slight reduction of EV numbers, the HRP-mediated signal appeared to be stable (Figure 4A). We also resuspended HRP⁺ EVs in an EV storage buffer (PBS/0.2% bovine serum albumin/25 mM Trehalose/25 mM HEPES, pH 7.0), suitable for long-term EV storage as described (Görgens et al. 2022) and stored the EVs at –80°C. EVs were thawed after 4 months and particle numbers and HRP activity were determined. No significant reduction of the enzymatic activity was observed, indicating the possibility for a long-term use of HRP⁺ EVs (Figure 4B). We furthermore separated fresh EVs and EVs thawed after 4 months at –80°C by size-exclusion chromatography (SEC) and measured the HRP activity in the EV-containing fractions to confirm that HRP is still associated with EVs after freezing (Figure S10).

Next, we wanted to examine the stability of the HRP activity in biological samples. For this, we spiked 100 μ L of human serum with 200 μ U of HRP⁺ EVs and incubated the mixture at 4°C and isolated EVs after 24, 48 and 72 h of incubation by using spin columns pre-packed with Sepharose CL-4B (Figures 4C and S2). The EV-containing fraction 2 was diluted in PBS (1–20 μ L/well out of 150 μ L total volume) and HRP activity was measured by adding TMB substrate. As indicated in Figure 4D, the incubation of HRP⁺ EVs in serum for up to 72 h prior to EV isolation did not affect the enzymatic activity of HRP.

3.5 | Comparison of HRP⁺ EVs to Commercially Available GFP⁺ EVs

We also compared HRP⁺ EVs to commercially available reference EVs carrying intraluminal GFP as a marker protein (Sigma-Aldrich, SAE0193; described in Geurickx et al. 2019). We resuspended these GFP⁺ EVs in PBS and determined their particle number by NTA. Then, we measured the fluorescent intensity of the GFP⁺ EVs with a plate reader equipped with a 488 nm laser. For this, we diluted the EVs in PBS, as depicted in Figure 5A. The GFP⁺ EVs could be detected at a LLoD of 1×10^8 . Next, we added different numbers of HRP⁺ EVs or GFP⁺ EVs to 100 μ L of serum (1×10^7 – 3×10^8 HRP⁺ EVs or 5×10^7 – 2.5×10^9 GFP⁺ EVs). After EV purification via SEC, the fluorescent signal of the GFP⁺ EVs (Figure 5C) and the absorbance of the HRP⁺ EVs after addition of TMB (Figure 5D) were measured with a plate reader. A linear correlation of 2.5×10^7 – 3×10^8 EVs for HRP⁺, and 5×10^8 – 2.5×10^9 EVs for GFP⁺ EVs was determined. These experiments demonstrate a more than ten-times higher sensitivity of enzyme-based HRP⁺ EVs detection over commercial GFP⁺ EVs (summarized in Figure 5B).

3.6 | HRP⁺ EVs Are Suitable for the Validation of EV Isolation Methods

Reference HRP⁺ EVs were used to determine the recovery rate of common EV isolation methods, including SEC, density gradient and commercial kits (ExoQuick, Exo-spin). For this, human serum samples were spiked with HRP⁺ EVs of known enzymatic activity prior to EV isolation. The HRP signal was measured before (input) and after (output) SEC and used to calculate the recovery rate. In the example depicted in Figure 6A, 500 μ U of HRP⁺ EVs were spiked into 200 μ L of serum and the EVs

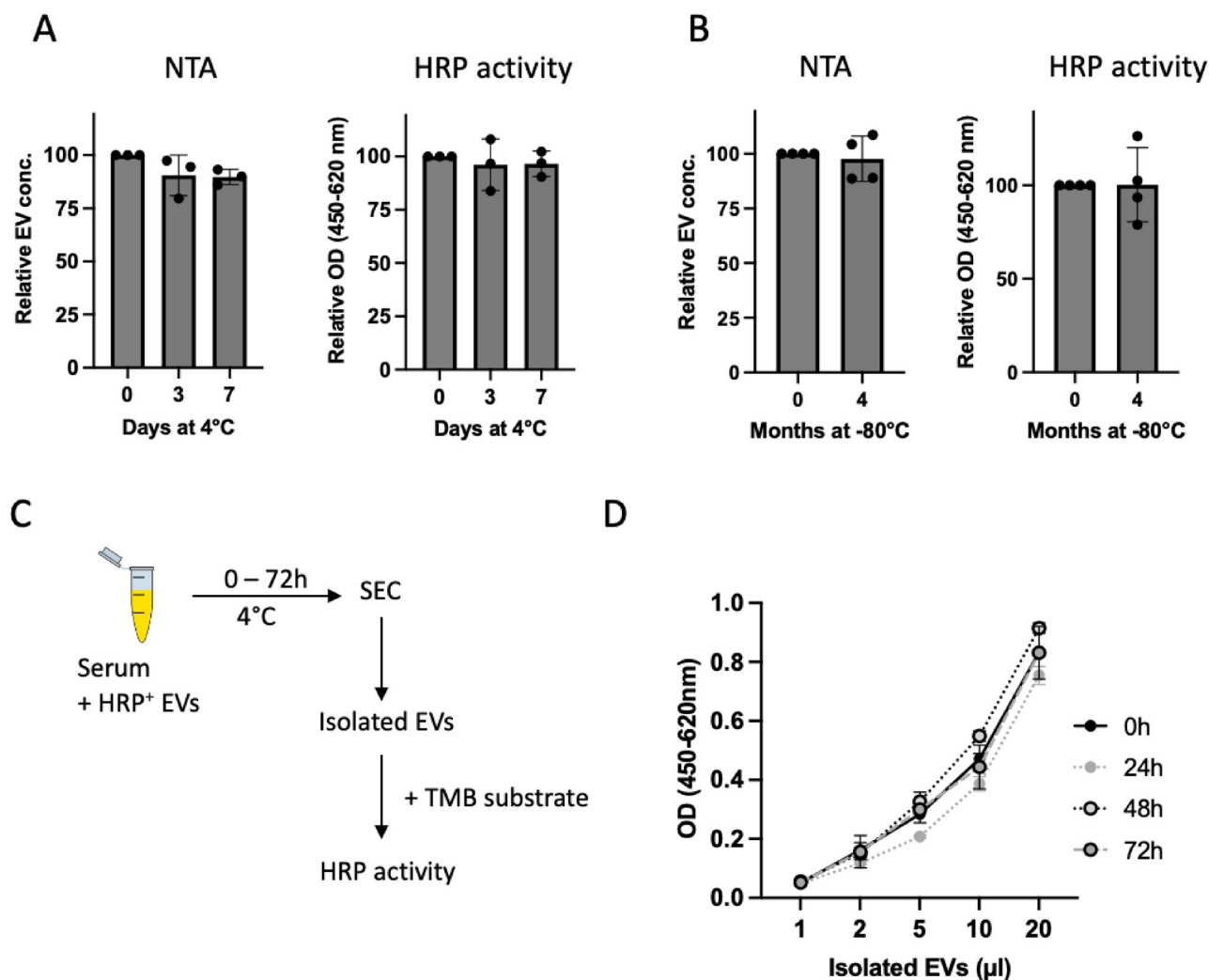


FIGURE 4 | Stability of HRP⁺ EVs during storage and in human serum. HRP⁺ EVs purified by ultracentrifugation were stored at 4°C and at -80°C. (A) Relative EV concentration and HRP activity were assessed after storing the EVs in PBS at 4°C for 3 and 7 days ($n = 3$). (B) EVs were mixed with EV storage buffer (PBS/0.2% serum albumin/25 mM Trehalose/25 mM HEPES, pH 7.0) and stored at -80°C. Particle concentration and HRP activity were measured after 4 months ($n = 4$). (C) HRP⁺ EVs were spiked into serum from a healthy individual. Specifically, 400 μ L serum were divided in four tubes and each was spiked with 200 μ L HRP⁺ EVs. The samples were kept at 4°C and serum EVs were isolated by SEC at the indicated four timepoints (0, 24, 48 or 72 h). A schematic representation of the experiment is shown. (D) The isolated EVs were diluted in triplicates as indicated, and HRP activity was measured by adding the TMB substrate. Reaction was stopped after 10 min.

were isolated by ExoQuick. Subsequently, the HRP signal was measured in the EV eluate (1–5 μ L of isolated EVs/well). The recovery was found to be about 87% according to the slope ratio that was calculated by dividing the slope of the linear regression of the output by the slope of the input signal (500 μ U HRP⁺ EVs in PBS).

We furthermore used HRP⁺ EVs to determine the percentage of recovery for other widely used EV isolation methods. For this, we pooled the EV-containing fractions 2 and 3 of a density gradient and fractions 7–9 after SEC. Recoveries of the different methods ranged from 49.5% (mini-SEC) to 76.5% (SEC qEV70) (Figure 6B). In addition to this inter-method variance, also substantial donor-to-donor variability was observed.

Using 200 μ L human serum from one donor spiked with different amounts of HRP⁺ EVs (100–1000 μ U) prior to ExoQuick isolation,

we also tested whether this parameter affected the recovery rate, which was not the case. A linear correlation spanning one order of magnitude between the enzymatic activity of the HRP⁺ EVs and the measured OD in 5 μ L of the EV eluate was observed (Figure 6C).

To validate the reproducibility of HRP detection following EV isolation, 1000 μ U of HRP⁺ EVs were mixed with 200 μ L of human serum in five technical replicates by two different operators. They independently performed ExoQuick isolation and determined the percentage of recovery. The mean recoveries were $48 \pm 3.3\%$ for operator 1 and $45 \pm 5.0\%$ for operator 2 (Figure 6D). The inter-assay variation, represented by the coefficient of variation, a measure of the dispersion of data points around the mean was 6.9% and 11.1% for operator 1 and 2, respectively. We also measured the concentration of isolated serum EVs by NTA after EV isolation using the ExoQuick, mini-SEC or density gradient purification

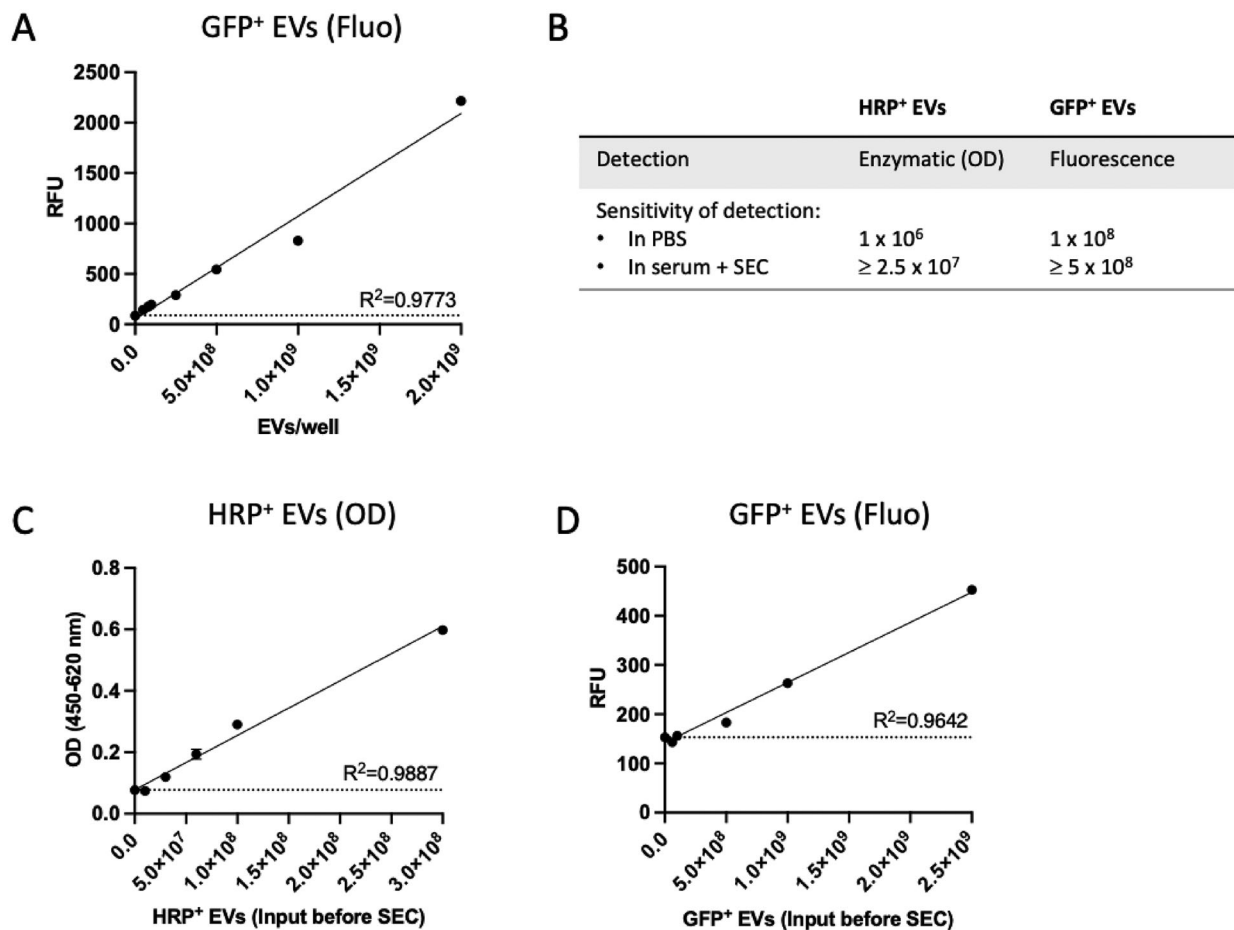


FIGURE 5 | Detection of HRP⁺ EVs in comparison with commercially available GFP⁺ reference EVs. (A) GFP⁺ EVs purchased from Sigma–Aldrich were diluted in PBS and transferred to a 96-well cluster plate. Fluorescence was measured with a CLARIOstar plate reader. The dotted line represents the blank value (PBS only); RFU, relative fluorescence units. (B) Table summarizing the detection and sensitivity for HRP⁺ EVs and GFP⁺ EVs. (C) Different amounts of HRP⁺ EVs (0.3 to 3×10^8 particles) were spiked into $100 \mu\text{L}$ serum and EVs were subsequently purified by using Sepharose 4-CL mini spin columns. The HRP activity in the eluates was measured by adding TMB substrate and the values were plotted against the numbers of HRP⁺ EVs prior to SEC. The dotted line represents the serum only control. (D) A comparable experiment was performed with GFP⁺ EVs purchased from Sigma. Their fluorescence was determined after SEC.

methods. Normalization of the particle numbers based on the recovery rate of the HRP⁺ EVs led to a reduction of inter-assay variability from 22% to 16%, 16% to 3% and 18% to 4%, respectively (Figure 6E and Table S1).

4 | Discussion

The poorly established and infrequent use of universal reference EVs is a significant shortcoming in the field that hinders scientific progress and interferes with clinical applications of EVs. Therefore, reliable tools for normalization and standardization are urgently needed, especially for the development of EV-based diagnostics.

In this study we introduce a new class of cell culture-derived EVs exposing HRP on their surface. The detection of these EVs via the enzymatic activity of HRP represents a highly sensitive and robust system, which can be used to (1) trace EVs through various isolation methods, (2) standardize protocols and SOPs, (3) calculate the yield after isolation, (4) back-calculate the

total EV numbers in biological and medical samples and cell culture supernatants and (5) normalize clinical specimens prior to diagnostic downstream analyses.

Derived from HEK293 cells, our reference EVs have a biochemical composition and biophysical properties comparable to EVs secreted from other human cell lines and EVs present in biological samples, such as serum or plasma. They contain typical EV marker proteins (such as CD63, CD81, Tsg101 or Alix), are homogeneous in size and float at the expected specific density in sucrose gradients. Despite these common attributes, HRP⁺ EVs are clearly distinguishable from EVs in biological or medical samples as they carry a plant-based enzyme, which is absent from human samples. Hence, the HRP protein or the corresponding mRNA are exclusive and specific components of HRP⁺ EVs, which allow for the background-free and sensitive tracing of EV preparations. By exploiting the enzymatic activity of HRP and measuring substrate turnover in spiked samples, the HRP⁺ EVs can be easily detected and tracked during most purification processes. Importantly, the activity of the EV-associated HRP enzyme remains stable upon freezing and thawing.

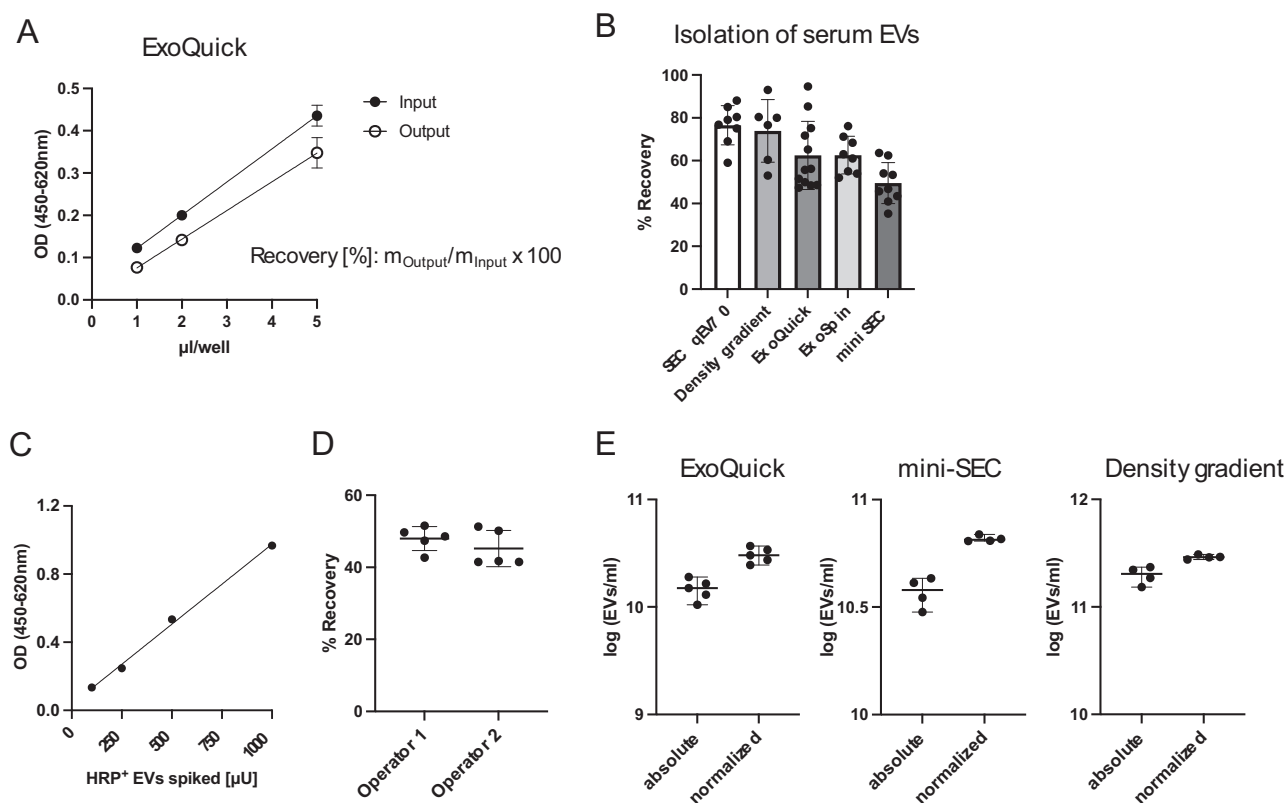


FIGURE 6 | HRP⁺ EVs can be used to determine the recovery efficiencies of common EV isolation methods. (A) 500 μU of HRP⁺ EVs were spiked into 200 μL human serum and EV isolation was performed using the ExoQuick kit. According to the manufacturer's protocol the EVs were eluted with 500 μL elution buffer. In parallel, 500 μL of PBS were mixed with the same amount of HRP⁺ EVs, serving as input control. 1, 2 and 5 μL of isolated EVs (Output) and PBS/EV mix (Input) were transferred to a microtiter plate in a final volume of 50 μL PBS. 50 μL of TMB substrate were added and the reaction was stopped after 10 min. As indicated, the recovery rate can be calculated by using the slopes of the linear regression curves. (B) Serum EVs from different human donors were isolated by using different methods, including qEV70 SEC, iodixanol gradient, ExoQuick, ExoSpin and mini-SEC methods. The percentages of recovery were calculated by comparing the output and input HRP signals. (C) 500 μL serum was spiked with different amounts of HRP⁺ EVs (100–1000 μU) prior to EV isolation using the ExoQuick kit. The HRP activity was determined in 5 μL of the EV eluate. $R^2 = 0.9965$. (D) The isolation of serum EVs from one donor by ExoQuick was performed in five technical replicates by two different operators. The recoveries were calculated using spike-in HRP⁺ reference EVs. (E) The number of EVs was measured by NTA after EV isolation by ExoQuick ($n = 5$), mini-SEC or density gradient centrifugation ($n = 4$). The recovery was determined by measuring the HRP activity in the same tube with spiked HRP⁺ reference EVs and was used to normalize the corresponding absolute EV number. Source data can be found in Table S1.

In the present study, we used the chromogenic substrate TMB and fluorogenic Amplex UltraRed reagent to detect HRP⁺ EVs with a standard absorbance plate reader, but other inexpensive and sensitive substrates are also commercially available (Dunford and Jones 2010; Veitch 2004). The choice of substrate depends on the required assay sensitivity, the type of read-out needed, but also on the instrumentation available for signal detection. Therefore, the usage of reference EVs based on HRP can be easily implemented in the laboratory without the need for costly reagents and instruments.

Monitoring HRP⁺ EVs in spike-in experiments can be conducted in different ways, depending on the preferred assay system and read-out. By adding HRP substrate directly to samples containing HRP⁺ EVs, the signal can be rapidly measured and allows assessment of EV quantity and yield. Additionally, the surface-anchored HRP is also accessible to antibody-mediated detection and immobilization using HRP-specific antibodies, which enables the usage of antibody-based methods like ELISA,

fluorescent NTA or sensitive nano-flow cytometry. We were furthermore able to detect HRP mRNA in spiked EV preparations, indicating that HRP⁺ EVs are also suitable as internal control for RNA-based read-outs (Figure S11). Further investigations will be required to support this aspect.

We also compared HRP⁺ EVs to previously published reference GFP⁺ EVs which can be traced and quantified using fluorescence-based technologies (Geeurickx et al. 2019). Detection of both GFP⁺ and HRP⁺ EVs was equally simple to perform and only requires basic instrumentation. However, in our hands, the measurement of HRP⁺ EVs turned out to be much more sensitive so that significantly smaller numbers of EVs were required for, for example, spike-in experiments. Also, HRP readily accepts different substrates allowing for the development of a wide panel of assays and read-out options.

We investigated the application of HRP⁺ EVs in spike-in experiments and in in vitro tracking to evaluate recovery efficiencies

and the performance of different EV isolation methods. The number of spiked EVs should be adapted according to the detection method. We do recommend using a minimum of 1000 μ U of HRP⁺ EVs per mL serum or other biological fluids and to sample 1%–5% of the volume that contains the isolated or processed EVs to measure HRP activity to deduce and calculate the percentage of HRP⁺ EVs recovered. Naturally, EV isolation from biological samples is subject to variations due to the choice of the technique, the consumables used (e.g., EVs may stick to the surface of certain plastic tubes), operator-dependent handling and donor-to-donor variability, all of which result in low reproducibility and variable recovery rates (Brennan et al. 2020; Torres Crigna et al. 2021; Van Deun et al. 2017; Williams et al. 2023). By using HRP⁺ EVs, we introduce a new possibility to optimize and control EV-based methods and perform intra- and inter-experimental normalization and standardization.

HRP is a stable and reliable oxidizing enzyme with a long shelf life that allows rapid detection of signal outputs. Nevertheless, different factors in an experiment can interfere with the HRP measurement. Especially complex biological samples, such as serum and plasma may influence the performance of the HRP⁺ EV detection and proper controls should be included in every experiment. For example, we observed that unprocessed pure serum contains protein factors that can inhibit HRP activity (Figure S12). Therefore, HRP⁺ EVs should not be measured in pure serum directly. Fortunately, this effect is reversible and can be overcome by either diluting the serum (1:50 or higher) or, as shown in this study, by EV isolation in order to separate EVs from the interfering serum protein components of unidentified nature. Similarly, we do not recommend to use the HRP⁺ EVs in undiluted urine samples (Campbell et al. 2014) (Figure S12C).

In conclusion, we describe a new class of reference EVs that can be traced and detected with a simple yet very sensitive enzymatic reaction. We developed HRP⁺ EVs to foster standardization and harmonization in the EV field for both scientific application and routine clinical use. We are currently evaluating additional applications, for example, by integrating tumour markers into the surface of the HRP⁺ EVs. In this way, the EVs could serve as ideal controls and inter-assay calibrators for the development, standardization and normalization of customized diagnostic assays. Since we only introduce a few examples of application in the present study, we do encourage the readers to test and make use of the reference EVs according to their own needs and ideas.

Author Contributions

Daniela Waas: investigation (lead), methodology (equal). **Marc Juraschitz:** investigation (supporting), methodology (supporting), project administration (equal), writing – review and editing (supporting). **Yen-Fu Adam Chen:** investigation (supporting), methodology (equal). **Harald Waltenberger:** validation (supporting), writing – review and editing (supporting). **Wolfgang Hammerschmidt:** conceptualization (equal), supervision (supporting), visualization (supporting), writing – review and editing (lead). **Reinhard Zeidler:** conceptualization (equal), writing – review and editing (supporting). **Sonja Molinaro:** conceptualization (supporting), resources (lead). **Kathrin Gärtner:** project administration (equal), supervision (lead), visualization (lead), writing – original draft (lead).

Acknowledgements

We thank Josef Mautner, Helmholtz Centre Munich, for providing the HEK293 suspension cell line. We also would like to acknowledge the use of the JEM-1400Plus TEM and technical assistance by Carsten Peters at the TUM Electron Microscopy Core Facility, Technical University of Munich, Garching.

Conflicts of Interest

K.G., S.M. and M.J. are inventors on a patent application assigned to Eximmium Biotechnologies and Microcoat for the usage of HRP⁺ EVs (WO2024089180). K.G. is a shareholder and employee of Eximmium Biotechnologies. S.M. is a shareholder of Microcoat, W.H. and R.Z. are shareholders of Eximmium Biotechnologies. The other authors declare no competing interests.

Data Availability Statement

The data that support the findings of this study are available from the corresponding author upon reasonable request.

References

- Azevedo, A. M., V. C. Martins, D. M. F. Prazeres, V. Vojinović, J. M. S. Cabral, and L. P. Fonseca. 2003. *Horseradish Peroxidase: A Valuable Tool in Biotechnology*, Vol. 9, 199–247. Elsevier. [https://doi.org/10.1016/S1387-2656\(03\)09003-3](https://doi.org/10.1016/S1387-2656(03)09003-3).
- Becker, A., B. K. Thakur, J. M. Weiss, H. S. Kim, H. Peinado, and D. Lyden. 2016. “Extracellular Vesicles in Cancer: Cell-to-Cell Mediators of Metastasis.” *Cancer Cell* 30, no. 6: 836–848. <https://doi.org/10.1016/j.ccell.2016.10.009>.
- Brennan, K., K. Martin, S. P. FitzGerald, et al. 2020. “A Comparison of Methods for the Isolation and Separation of Extracellular Vesicles From Protein and Lipid Particles in Human Serum.” *Scientific Reports* 10, no. 1: 1039. <https://doi.org/10.1038/s41598-020-57497-7>.
- Campbell, K. L., M. Lopresti, and W. Lukas. 2014. “Inhibition of Horseradish Peroxidase (HRP) by a Nonhydrophobic Component of Urine: A Caution for Immunoassays.” *Open Clinical Chemistry Journal* 7, no. 1: 1–7. <https://doi.org/10.2174/1874241601407010001>.
- Dunford, H. B., and P. A. Jones. 2010. *Peroxidases and Catalases: Biochemistry, Biophysics, Biotechnology and Physiology*, 2nd ed. John Wiley and Sons Inc.
- Gärtner, K., M. Luckner, G. Wanner, and R. Zeidler. 2019. “Engineering Extracellular Vesicles as Novel Treatment Options: Exploiting Herpesviral Immunity in CLL.” *Journal of Extracellular Vesicles* 8, no. 1: 1573051. <https://doi.org/10.1080/20013078.2019.1573051>.
- Geeurickx, E., L. Lippens, P. Rappu, B. G. De Geest, O. De Wever, and A. Hendrix. 2021. “Recombinant Extracellular Vesicles as Biological Reference Material for Method Development, Data Normalization and Assessment of (Pre-)Analytical Variables.” *Nature Protocols* 16, no. 2: 603–633. <https://doi.org/10.1038/s41596-020-00446-5>.
- Geeurickx, E., J. Tulkens, B. Dhondt, et al. 2019. “The Generation and Use of Recombinant Extracellular Vesicles as Biological Reference Material.” *Nature Communications* 10, no. 1: 3288. <https://doi.org/10.1038/s41467-019-11182-0>.
- Görgens, A., M. Bremer, R. Ferrer-Tur, et al. 2019. “Optimisation of Imaging Flow Cytometry for the Analysis of Single Extracellular Vesicles by Using Fluorescence-Tagged Vesicles as Biological Reference Material.” *Journal of Extracellular Vesicles* 8, no. 1: 1587567. <https://doi.org/10.1080/20013078.2019.1587567>.
- Görgens, A., G. Corso, D. W. Hagey, et al. 2022. “Identification of Storage Conditions Stabilizing Extracellular Vesicles Preparations.” *Journal of Extracellular Vesicles* 11, no. 6: e12238. <https://doi.org/10.1002/jev2.12238>.
- Krainer, F. W., and A. Glieder. 2015. “An Updated View on Horseradish Peroxidases: Recombinant Production and Biotechnological

- Applications." *Applied Microbiology and Biotechnology* 99, no. 4: 1611–1625. <https://doi.org/10.1007/s00253-014-6346-7>.
- Li, K., Y. Chen, A. Li, C. Tan, and X. Liu. 2019. "Exosomes Play Roles in Sequential Processes of Tumor Metastasis." *International Journal of Cancer* 144, no. 7: 1486–1495. <https://doi.org/10.1002/ijc.31774>.
- Melo, S. A., L. B. Luecke, C. Kahlert, et al. 2015. "Glypican-1 Identifies Cancer Exosomes and Detects Early Pancreatic Cancer." *Nature* 523, no. 7559: 177–182. <https://doi.org/10.1038/nature14581>.
- Nawaz, M., G. Camussi, H. Valadi, et al. 2014. "The Emerging Role of Extracellular Vesicles as Biomarkers for Urogenital Cancers." *Nature Reviews Urology* 11, no. 12: 688–701. <https://doi.org/10.1038/nrurol.2014.301>.
- Sadovska, L., J. Eglitis, and A. Linē. 2015. "Extracellular Vesicles as Biomarkers and Therapeutic Targets in Breast Cancer." *Anticancer Research* 35, no. 12: 6379–6390.
- Tang, M. K. S., and A. S. T. Wong. 2015. "Exosomes: Emerging Biomarkers and Targets for Ovarian Cancer." *Cancer Letters* 367, no. 1: 26–33. <https://doi.org/10.1016/j.canlet.2015.07.014>.
- Théry, C., K. W. Witwer, E. Aikawa, et al. 2018. "Minimal Information for Studies of Extracellular Vesicles 2018 (MISEV2018): A Position Statement of the International Society for Extracellular vesicles and Update of the MISEV2014 Guidelines." *Journal of Extracellular Vesicles* 7, no. 1: 1535750. <https://doi.org/10.1080/20013078.2018.1535750>.
- Théry, C., L. Zitvogel, and S. Amigorena. 2002. "Exosomes: Composition, Biogenesis and Function." *Nature Reviews Immunology* 2, no. 8: 569–579. <https://doi.org/10.1038/nri855>.
- Torres Crigna, A., F. Fricke, K. Nitschke, et al. 2021. "Inter-Laboratory Comparison of Extracellular Vesicle Isolation Based on Ultracentrifugation." *Transfusion Medicine and Hemotherapy* 48, no. 1: 48–59. <https://doi.org/10.1159/000508712>.
- Valkonen, S., E. van der Pol, A. Böing, et al. 2017. "Biological Reference Materials for Extracellular Vesicle Studies." *European Journal of Pharmaceutical Sciences* 98: 4–16. <https://doi.org/10.1016/j.ejps.2016.09.008>.
- van Deun, J., P. Mestdagh, P. Agostinis, et al. 2017. "EV-TRACK: Transparent Reporting and Centralizing Knowledge in Extracellular Vesicle Research." *Nature Methods* 14, no. 3: 228–232. <https://doi.org/10.1038/nmeth.4185>.
- van Niel, G., G. D'Angelo, and G. Raposo. 2018. "Shedding Light on the Cell Biology of Extracellular Vesicles." *Nature Reviews Molecular Cell Biology* 19, no. 4: 213–228. <https://doi.org/10.1038/nrm.2017.125>.
- Varga, Z., E. van der Pol, M. Pálmai, et al. 2018. "Hollow Organosilica Beads as Reference Particles for Optical Detection of Extracellular Vesicles." *Journal of Thrombosis and Haemostasis* 16, no. 8: 1646–1655. <https://doi.org/10.1111/jth.14193>.
- Veitch, N. C. 2004. "Horseradish Peroxidase: A Modern View of a Classic Enzyme." *Phytochemistry* 65, no. 3: 249–259. <https://doi.org/10.1016/j.phytochem.2003.10.022>.
- Wang, L., W. Zhao, and W. Tan. 2008. "Bioconjugated Silica Nanoparticles: Development and Applications." *Nano Research* 1, no. 2: 99–115. <https://doi.org/10.1007/s12274-008-8018-3>.
- Welsh, J. A., E. van der Pol, B. A. Bettin, et al. 2020. "Towards Defining Reference Materials for Measuring Extracellular Vesicle Refractive Index, Epitope Abundance, Size and Concentration." *Journal of Extracellular Vesicles* 9, no. 1: 1816641. <https://doi.org/10.1080/20013078.2020.1816641>.
- Williams, S., M. Fernandez-Rhodes, A. Law, B. Peacock, M. P. Lewis, and O. G. Davies. 2023. "Comparison of Extracellular Vesicle Isolation Processes for Therapeutic Applications." *Journal of Tissue Engineering* 14: 1–13. <https://doi.org/10.1177/20417314231174609>.
- Witwer, K. W., E. I. Buzás, L. T. Bemis, et al. 2013. "Standardization of Sample Collection, Isolation and Analysis Methods in Extracellular Vesicle Research." *Journal of Extracellular Vesicles* 2, no. 1: 20360. <https://doi.org/10.3402/jev.v2i0.20360>.

Zhang, C., C. Qin, S. Dewanjee, et al. 2024. "Tumor-Derived Small Extracellular Vesicles in Cancer Invasion and Metastasis: Molecular Mechanisms, and Clinical Significance." *Molecular Cancer* 23, no. 1: 18. <https://doi.org/10.1186/s12943-024-01932-0>.

Supporting Information

Additional supporting information can be found online in the Supporting Information section.

Supplementary Figure 1: Representative illustration of serum EV purification by size exclusion chromatography using the qEVoriginal column. **Supplementary Figure 2:** Isolation of serum EVs was performed by SEC with mini spin columns packed with Sepharose CL-4B. **Supplementary Figure 3:** Evaluation of optimal hemin concentration for HEK293-HRP⁺ suspension cells. **Supplementary Figure 4:** Transmission electron microscopy of HRP⁺ extracellular vesicles purified from conditioned cell culture supernatant by serial centrifugation. **Supplementary Figure 5:** Size of EVs isolated from different sources was determined by NTA. **Supplementary Figure 6:** Characterization of HRP⁺ EVs purified by density gradient centrifugation. **Supplementary Figure 7:** Characterization of HEK293-derived EVs by high-sensitivity flow cytometry. **Supplementary Figure 8:** Treatment of purified HRP⁺ EVs with Proteinase K (PK) confirms surface association of the enzyme. **Supplementary Figure 9:** Measurement of EV-associated and free HRP activity using the fluorogenic substrate Amplex Red. **Supplementary Figure 10:** Purified HRP⁺ EVs were loaded onto an Izon qEV70 SEC column and fractions of 500 μ L were collected. **Supplementary Figure 11:** Analysis of HRP and GAPDH RNA in EVs. A: RNA was isolated from HEK293-wt and HEK-HRP EVs and transcribed into cDNA. **Supplementary Figure 12:** High concentrations of protein components in pure serum and urine samples can inhibit the activity of EV-associated HRP. **Supplementary Figure 13:** Uncropped images corresponding to the Western blots shown in Figures 1D and 3D. **Supplementary Table 1:** HRP⁺ reference EVs were spiked into serum and EV purification was performed in technical replicates with the indicated methods.